



OPEN

Metasequoia glyptostroboides potentiates anticancer effect against cervical cancer via intrinsic apoptosis pathway

Hoomin Lee^{1,5}, Cheolwoo Oh^{1,5}, Suji Kim¹, Debasish Kumar Dey², Hyung Kyo Kim³, Vivek K. Bajpai⁴✉, Young-Kyu Han⁴✉ & Yun Suk Huh¹✉

This study was undertaken to investigate the anticancer effects of organic extracts derived from the floral cones of *Metasequoia glyptostroboides*. Dried powder of *M. glyptostroboides* floral cones was subjected to methanol extraction, and the resulting extract was further partitioned by liquid–liquid extraction using the organic solvents *n*-hexane, dichloromethane (DME), chloroform, and ethyl acetate in addition to deionized water. HeLa cervical and COS-7 cells were used as a cancer cell model and normal cell control, respectively. The anticancer effect was evaluated by using the Cell Counting Kit-8 assay. The viability of COS-7 cells was found to be 12-fold higher than that of the HeLa cells under the administration of 50 µg/ml of the DME extract. Further, the sub-G1 population was determined by FACS analysis. The number of cells at the sub-G1 phase, which indicates apoptotic cells, was increased approximately fourfold upon treatment with the DME and CE extracts compared with that in the negative control. Furthermore, RT-qPCR and western blotting were used to quantitate the relative RNA and protein levels of the cell death pathway components, respectively. Our results suggest that the extracts of *M. glyptostroboides* floral cones, especially the DME extract, which possesses several anticancer components, as determined by GC–MS analysis, could a potential natural anticancer agent.

Cervical cancer affects many women in developing countries and has a high mortality rate. Although the cervical cancer screening program has reduced the incidence and mortality of cervical cancer, the incidence among young women remains a public health problem¹. In addition, the administration of chemotherapeutic agents and multi-drug resistance are accompanied by severe side effects that cause negative gynecological and obstetric outcomes^{2,3}.

Tumor cells in the ovary can metastasize to the lymphatic and circulatory systems if not blocked by the anatomical barriers⁴. Surgical resection and systemic chemotherapy can affect drug efficacy. Consequently, high chemotherapeutic doses that are adversary to human health are the only options to treat the mucosal and epithelial membranes of the affected tissues. Doxorubicin (DOX) is an efficient chemotherapeutic agent that is widely used for the treatment of various cancers⁵. However, adversary side effects, poor bio-distribution, and high toxicity to non-cancerous cells limit the use of DOX^{6,7}.

Targeting apoptosis avoidance, a major feature of cancers, is the most effective nonsurgical strategy for the treatment of cancers because it is not specific to the cause or type of cancer⁸. Apoptosis is mediated by an intrinsic or extrinsic pathway based on the origin of the apoptotic stimulus. These pathways are also known as mitochondrial and death receptor pathways, respectively⁸. The intrinsic apoptosis pathway is activated inside the cell by the Bcl-2 protein family and is independent of receptor signal transduction^{8,9}. The extrinsic pathway is primarily mediated by the signaling through membrane-bound receptors belonging to the tumor necrosis factor (TNF) superfamily called the “death domain”⁹.

Metasequoia glyptostroboides Miki ex Hu (*M. glyptostroboides*) is a deciduous conifer from the red-wood family of Cupressaceae and is distributed in Europe as well as many parts of East Asia and North America¹⁰.

¹Department of Biological Engineering, NanoBio High-Tech Materials Research Center, Inha University, 100 Inha-ro, Nam-gu, Incheon 22212, Republic of Korea. ²Department of Biotechnology, Daegu University, Gyeongsan 38453, Republic of Korea. ³Department of Biomaterials Research Center, GENPEAU Corporation, Incheon 21990, Republic of Korea. ⁴Department of Energy and Materials Engineering, Dongguk University-Seoul, 30 Pildong-ro 1-gil, Seoul 04620, Republic of Korea. ⁵These authors contributed equally: Hoomin Lee and Cheolwoo Oh. ✉email: vbiotech04@gmail.com; ykenergy@dongguk.edu; yunsuk.huh@inha.ac.kr

Floral cone of *Metasequoia glyptostroboides* (222.9 g)

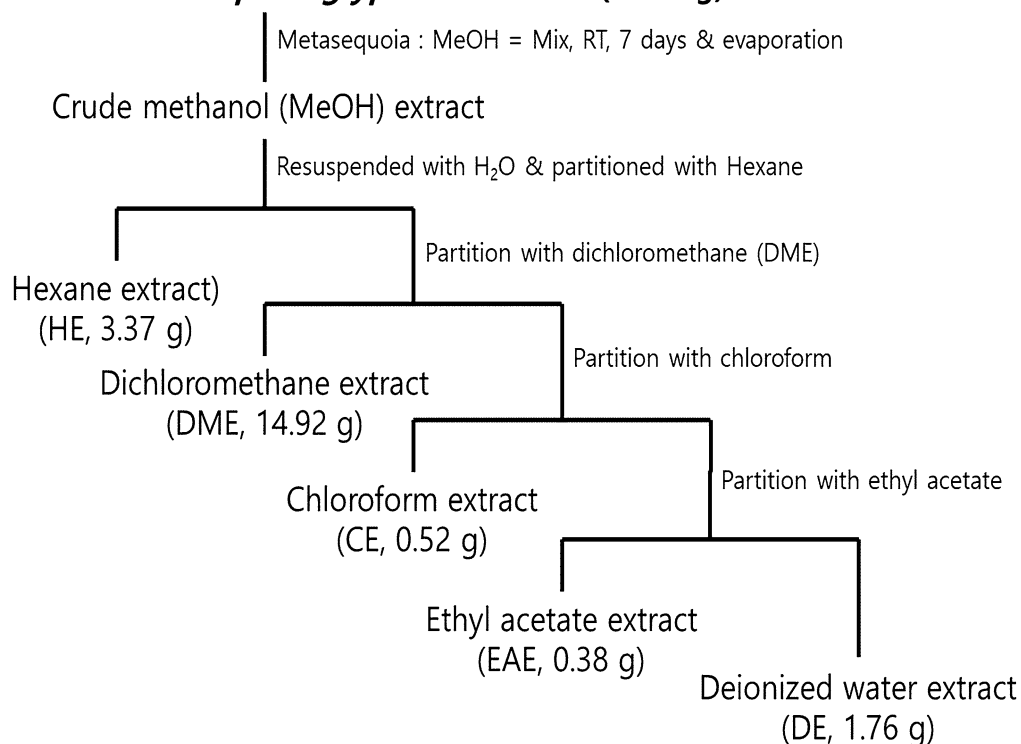


Figure 1. Partition of different solvent extracts through liquid–liquid extraction.

Herbal plant-based extracts have shown enormous potential in the treatment of various diseases, including cervical cancer. Although *M. glyptostroboides*-derived extracts or secondary metabolites have been found to exhibit numerous biological and pharmacological activities^{11–13}, the effect of *M. glyptostroboides* floral cone extracts on cervical cancer has not been addressed to date.

Therefore, in this study, *M. glyptostroboides* floral cone extracts prepared with various organic solvents were assessed for their anticancer effects on the cervical cancer cell line HeLa cells versus their normal counterparts, COS-7 cells. Also, chemical component analysis of the DME extract was performed using GC–MS analysis.

Methods

Materials. The organic solvents *n*-hexane, dichloromethane, chloroform, and ethyl acetate were purchased from Daejung (Korea). Dulbecco's Modified Eagle's Medium (DMEM), penicillin/streptomycin, fetal bovine serum (FBS), phosphate-buffered saline (PBS), and trypsin were purchased from Gibco (Carlsbad, CA). The Cell Counting Kit-8 (CCK-8) was purchased from Dojindo Co. Ltd. (Beijing, China).

Sample preparation. The floral cone powder of *M. glyptostroboides* was subjected to methanol extraction at a ratio of 1:10 (w/v) for 1 week and then filtered through a 0.45- μ m Whatman No. 1 filter paper. The supernatant was dried using a rotary evaporator (N-1110S-W, Eyela, Tokyo, Japan), resulting in the crude methanol extract (ME) of *M. glyptostroboides* floral cones with a yield of 9.40%. To prepare different organic extracts, ME was further dissolved in deionized (DI) water and successively partitioned using *n*-hexane (HE), dichloromethane (DME), chloroform (CE), and ethyl acetate (EAE) solvents. Each solvent layer was separated and dried using a rotary evaporator, resulting in the crude HE, DME, CE, and EAE extracts of *M. glyptostroboides* floral cones. To prepare the test samples, each extract sample was dissolved in dimethyl sulfoxide (DMSO). A detailed extraction procedure is provided in Fig. 1.

Cell cultures. HeLa (Human cervical carcinoma cell) and COS7 (African green monkey kidney cell) cells were cultured in DMEM medium with 10% FBS and 1% penicillin/streptomycin. Cells were incubated at 37 °C in humidified air with 5% CO₂.

Gas chromatography-mass spectroscopy (GC–MS) analysis. GC–MS analysis of DME extract was performed using a GC-Thermo Jeol JMS700 apparatus following our previously reported method, and components were identified using GC–MS-based NIST and Willey library¹⁴.

Cytotoxicity assay. For cytotoxicity assay, COS7 and HeLa cells were incubated with various concentrations of HE, DME, CE, EAE, and DE extracts of *M. glyptostroboides* floral cones. After 24 h incubation, cells were

washed with PBS three times. Then, the cell viability was measured using a CCK-8 cell counting kit following the manufacturer's protocol.

Nuclear fragmentation analysis. Hoechst staining¹⁵ was performed to examine the nuclear fragmentation effect of HE, DME, CE, EAE, and DE extracts of *M. glyptostroboides*. The HeLa cells were grown in 12-well-plate and treated with 50 µg/ml of HE, DME, CE, EAE, and DE extracts for 24 h. Finally, cells were treated with 1 µg/ml of Hoechst 33342 stain. After 15 min staining cells were washed with PBS (pH 8) and visualized under EPI fluorescence microscope (Nikon, Japan) and apoptotic index was calculated as the percentage of apoptotic nuclei compared to the total number of cells¹⁵.

Quantification of sub-G1 phase by flow cytometry analysis (FACS). FACS analysis was carried out to determine the cytotoxic effect of HE, DME, CE, EAE, and DE extracts of *M. glyptostroboides*. The sub-G1 population was quantified using propidium iodide (PI; Sigma-Aldrich) staining and a cellometer. HeLa cells were seeded in 6-well plates at a density of 1×10^6 cells per well, cultured for 24 h and then treated with 50 µg/ml of the HE, DME, CE, EAE, or DE extract for 24 h. Cells were harvested with trypsinization and fixed with 80% cold ethanol in PBS for 30 min. Cells were then washed twice with cold PBS and centrifuged at 2000 rpm. The pellet was resuspended in PBS and stained with 50 µg/ml PI in PBS containing 100 µg/ml RNase A. Cells were then incubated at 37 °C for 40 min. Afterward, their DNA contents were analyzed using the cellometer instrument.

Western blot analysis. HeLa cells were pretreated with 50 µg/ml of the HE, DME, CE, EAE, or DE extract of *M. glyptostroboides* floral cones. Total protein was obtained by lysing the cells with RIPA buffer containing protease and phosphatase inhibitors (ThermoFisher Scientific, UK). Protein samples were subjected to SDS-PAGE and electro-transferred onto polyvinylidene difluoride membranes (Millipore, Burlington, MA). The membranes were blocked using 5% skim milk in Tris-buffered saline-Tween 20 (TBST). The membranes were incubated overnight at 4 °C with the primary antibodies and then washed with TBST. The membranes were subsequently treated with the appropriate secondary antibodies for 4 h. β-actin was used as an internal standard. Image J software was used to analyze the band intensities.

RT-qPCR analysis. The mRNA levels of apoptosis markers in HeLa cells were assessed using RT-qPCR. Total RNA was collected using the TRIzol reagent (Life Technologies, Carlsbad, CA) and reverse-transcribed using the PrimeScript RT reagent Kit (Takara Bio Inc., Kusatsu, Japan). The CFX96 system (Bio-Rad Laboratories, Hercules, CA) and iQ SYBR Green Supermix (Bio-Rad Laboratories) were used for qPCR. β-actin mRNA levels were used to normalize p53, B-cell lymphoma 2 (Bcl-2), and Bcl-2-associated X (BAX) mRNA levels. The $2^{-\Delta\Delta CT}$ method was used to determine the relative mRNA levels. The primer sequences used in this study are provided in Supplementary Table S1.

Detection of reactive oxygen species (ROS) generation. The detection of ROS generation assay was according to previous studies with some modification¹⁶. To detect ROS at chemical level, a 500 µl sample of 1 mM 2',7'-dichlorodihydrofluorescein diacetate (DCF-DA; 287810, MERCK MILLIPORE, German) was reacted with 10 mM NaOH (2 ml) for 30 min to achieve complete deacetylation in the darkroom. The mixture solution was then neutralized with 10 ml PBS. Each sample in PBS was mixed with DCF-DA solution and horseradish peroxidase (HRP; P8375, SIGMA, USA) (2.2 unit per ml) at a ratio of 1:1:1 and reacted in a darkroom for 30 min. Centrifugation proceeded at 13,000 rpm and 4 °C for 10 min. The supernatant solution was moved to a 96 well black plate and the fluorescence intensity of DCF was observed with excitation and emission wavelengths at 485 nm and 535 nm, respectively. The standard curve was obtained from a H₂O₂ solution.

Further, the generation of ROS at cellular level was evaluated using DCF-DA (Cellular ROS assay kit, Abcam). In the presence of HRP and H₂O₂, DCF-DA is converted to highly fluorescent 2',7'-dichlorodihydrofluorescein (DCF). The ROS assay was performed according to the supplier's instructions. The confluent cells incubated at the concentration of 50 µg/ml per extract for 6 h in 12-well cell plates were treated with 1 mM of H₂O₂ for 30 min. The cells were twice washed with PBS and incubated with 10 mM DCF-DA for 40 min at 37 °C in the dark. The cells were then washed twice with PBS and analyzed by a microplate reader at an excitation and emission wavelength of 485 nm and 530 nm, respectively.

Statistical analysis. The data presented as the mean ± standard deviation from three independent experiences was analyzed by student's t-test with a p-value of <0.01 considered as significant for the differences.

Results and discussion

GC-MS analysis of DME. GC-MS analysis of DME resulted in the identification of 45 different chemical compounds (Supplementary Table S2). The majority of compounds belonged to the organic acids, terpenes and phenolic compounds, especially terpenes and quinones such as ferruginol¹⁷, taxodione¹⁸ which contributed significant amount of the total chemical composition of DME by 14.58 and 2.21%, respectively. The anticancer activities of these compounds are mediated due to the presence of hydroxyl groups^{17,18}, including other biologically active components, which have been reported to be anticancerous and/or antitumor in nature such as estradiol¹⁹. The results of GC-MS analysis of DME confirms that the reported anticancer activity of DME could be mediated via these bioactive components present in the DME.

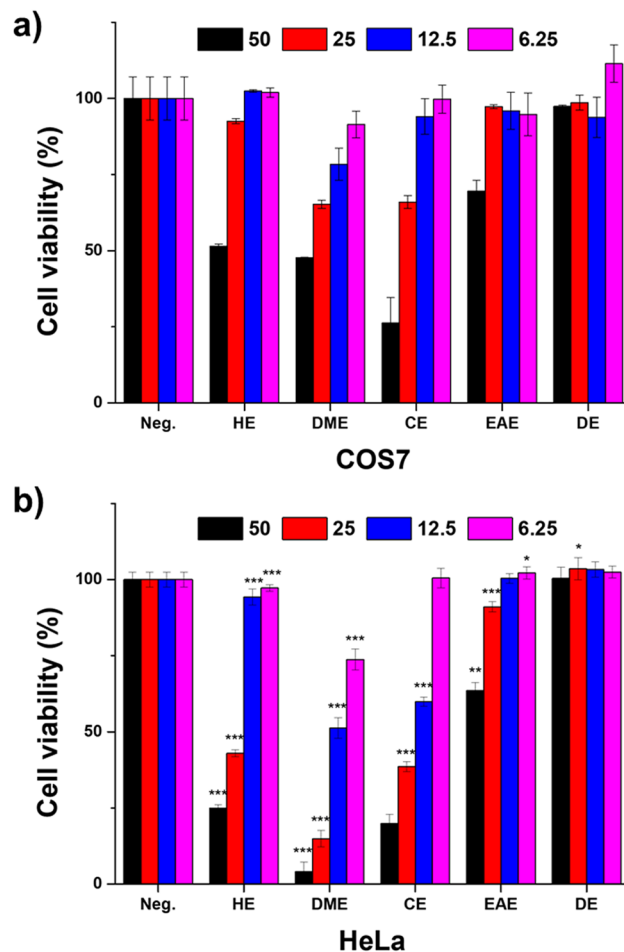


Figure 2. Anticancer effects of various extracts of *M. glyptostrobooides*. (a) COS7 and (b) HeLa cells were incubated for 24 h with *M. glyptostrobooides* extracts at 50, 25, 12.5, and 6.25 µg/ml. *** $p < 0.001$ indicate statistical significances compared to COS7.

Anticancer activities of *M. glyptostrobooides* extracts. The five organic extracts such as HE, DME, CE, EAE, and DE of *M. glyptostrobooides* floral cones were obtained via liquid–liquid extraction of the methanol extract. In brief, dried powder of the floral cones of *M. glyptostrobooides* was successively extracted with methanol and partitioned using the organic solvents *n*-hexane, dichloromethane, chloroform, and ethyl acetate in addition to DI water (Fig. 1). The cytotoxic effects of the extracts on HeLa cervical cancer cells were assessed for alongside COS7 cells as the non-cancer cell control using CCK-8. Cells were treated with the HE, DME, CE, EAE, and DE extracts for 24 h at the concentration range of 6.25, 12.5, 25, and 50 µg/ml per extract. Figure 2a,b show that the HE, DME, and CE extracts had considerable anticancer effects on HeLa cells in a dose-dependent manner. The viability of COS7 cells was 2-, 12-, and 1.3-fold higher than that of HeLa cells under the administration of 50 µg/ml of HE, DME, and CE extracts, respectively. We also confirmed low cytotoxicity of our test samples on normal cervical epithelial cells than HeLa cells (Supplementary Fig. S1). The IC_{50} values of HeLa and COS7 for HE, DE, and CE extracts were (31.89 and 52.11 µg/ml), (13.71 and 45.37 µg/ml) and (18.85 and 35.83 µg/ml), respectively, showing stronger toxicity to HeLa cells (Fig. 2). On the other hand, EAE and DE extracts did not show any difference in the cytotoxicity levels of both the tested cells lines. Previous studies have also shown the cytotoxic potentials of various plant extracts in several cancer lines including HeLa cells^{20,21}.

Quantification of sub G1 phase and nuclear disruption in HeLa cells. To assess the anticancer effects of various organic extracts of *M. glyptostrobooides* on HeLa cells, we performed Hoechst 33342 staining and cell cycle assay. Figure 3 shows the results of the Hoechst 33342 staining of HeLa cells treated with *M. glyptostrobooides*-derived extracts. The extracts DME and CE displayed a brightly colored condensed fragmented nuclei indicated nuclear disintegration and suggesting the apoptotic cell death²². In contrast to this, the extracts HE, EAE, and DE did not show the presence of apoptotic nuclei. Further, staining results were quantified as apoptotic index, suggesting $36.67 \pm 4.93\%$ and $28.66 \pm 3.79\%$ apoptotic nuclei in the cells treated with DME and CE, respectively. Moreover, the phenotypic characteristic of irregular cell morphologies and membrane blebbing especially in the DME and CE extracts treated cells indicated the apoptotic morphology (Fig. 3). These results

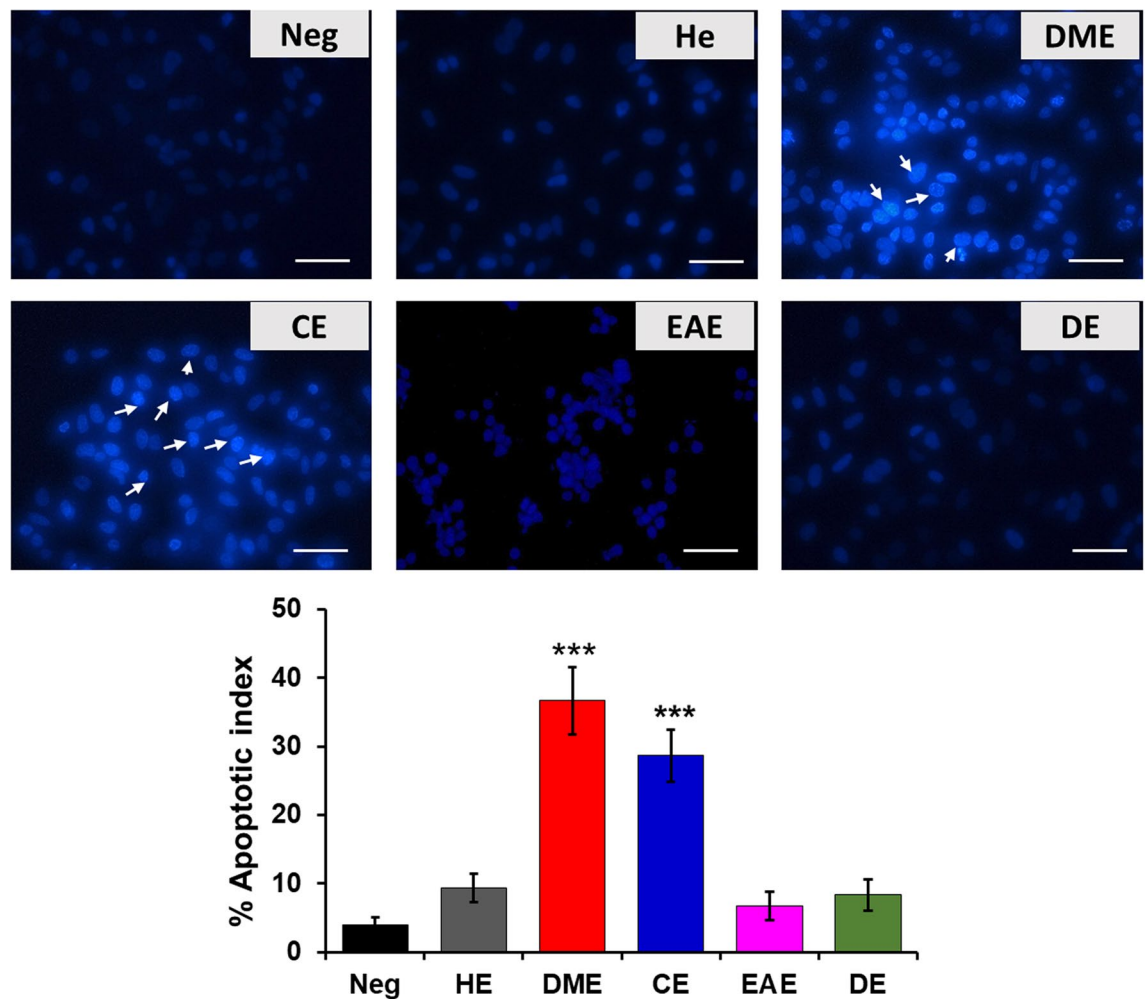


Figure 3. Effects of *M. glyptostroboides* extracts on the nuclei of HeLa cells. HeLa cells were incubated with *M. glyptostroboides* extracts of 50 $\mu\text{g}/\text{ml}$ for 24 h. Apoptotic cells indicated as bright colored condensed and fragmented nuclei stained with Hoechst 33342 (marked by arrow).

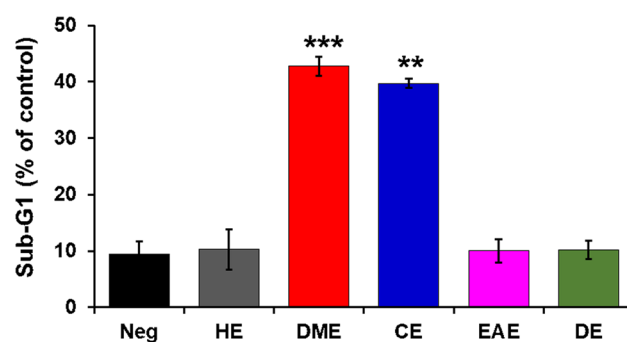


Figure 4. Apoptotic effect of *M. glyptostroboides* extracts examined by FACS. HeLa cells incubated with *M. glyptostroboides* extracts of 50 $\mu\text{g}/\text{ml}$ for 24 h and apoptosis was analyzed as the sub-G1 fraction by FACS. ** $p < 0.01$ and *** $p < 0.001$ indicates statistical significances compared to negative control.

are consistent with the results of the cell viability assay shown in Fig. 1, suggesting that the extracts induced apoptosis in HeLa cells.

To assess the anticancer effects of various organic extracts of *M. glyptostroboides* on HeLa cells, sub-G1 phase of cell cycle was determined by using PI-staining (Fig. 4 and Supplementary Fig. S2). PI can permeate through the damaged membranes of apoptotic cells and stains the nuclei^{23,24}. Apoptotic cells accumulate in the sub-G1 phase. The proportion of the cells in the sub-G1 phase upon treatment with the DE extract was $10.2 \pm 1.6\%$ and

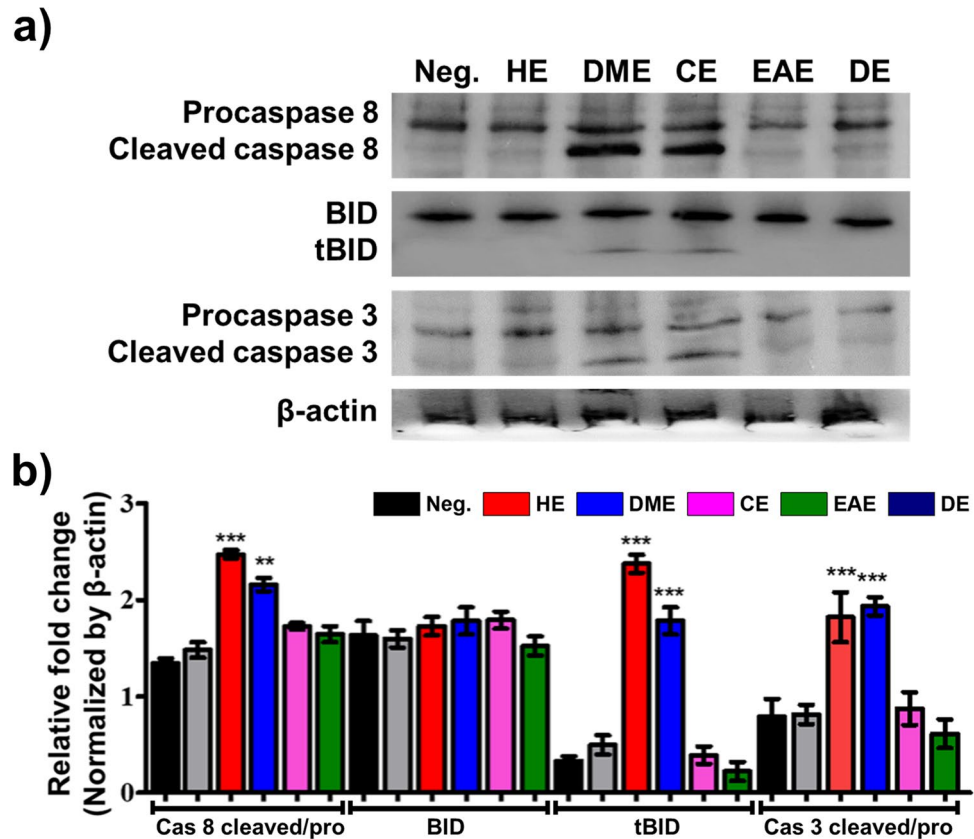


Figure 5. Evaluation of the apoptosis-related protein levels in HeLa cells treated with extracts of *M. glyptostroboides* extracts (50 µg/ml). **(a)** Western blot analysis and **(b)** Densitometry quantification of the respective proteins was evaluated by Image J software, and results were normalized with β-actin. ** $p < 0.01$ and *** $p < 0.001$ indicates statistical significances compared to negative control.

similar to that in the negative control ($9.4 \pm 2.3\%$), HE ($10.3 \pm 3.6\%$), and EAE ($10.03 \pm 2.1\%$). The maximum sub-G1 population was observed in DME ($42.76 \pm 1.7\%$) followed by CE ($39.7 \pm 0.81\%$), which was significantly 4.5- and 4.2-folds higher compared with the negative control (Fig. 4). Collectively, the results of the cell cycle analysis, cell viability assay, (Fig. 2b), and Hoechst 33342 staining showed that the DME and CE extracts induced apoptosis, suggesting the anticancer behavior of these extracts. These findings are in strong accordance with a recent study in which a plant-derived secondary metabolite has been shown to induce cell cycle assay and consequent apoptosis in HeLa cells²⁰.

Analysis of the apoptotic pathway in HeLa cervical cancer cells. Apoptosis is an important cellular process, and it is divided into two main pathways—extrinsic and intrinsic. To identify the apoptotic pathway induced in HeLa cells by the *M. glyptostroboides* extracts, we performed western blotting to evaluate the changes in the protein levels of the extrinsic apoptosis pathway components BID, Cleaved Caspase (Cl Cas)-3, and Cl Cas-8. Cas-8 is the initiator of the extrinsic apoptosis pathway. Stimulation of the death receptor activates Cas-8, which then cleaves BID²⁵. Cleaved BID, also known as truncated BID (tBID), induces the intrinsic pathway. Figure 5b shows the quantification of the data from the western blot analysis of Fig. 5a. The Cl Cas-8 level increased approximately 2.4- and 2.1-folds in HeLa cells treated with the DME and CE extracts, respectively, relative to the level in the negative control. Upregulated Cl Cas-8 levels increased the cleavage of BID into tBID. As shown in Fig. 5b, the tBID levels in HeLa cells treated with the DME and CE extracts were 2.3-, and 1.7-fold more higher, respectively, which were significantly different than that in the negative control. The level of Cl Cas3, which is a member of the cysteine-aspartic acid protease family, was significantly increased in the cells treated with the DME and CE extracts relative to the level in the negative control. These results strongly support that the DME and CE extracts activate caspase-8 to induce apoptosis in HeLa cells via the extrinsic pathway. Also, the significantly higher amount of cleaved Parp, a well-known marker of DNA damage and apoptosis²⁶, was noticed in the cells treated with the DME and CE (Fig. 6), suggesting the apoptotic potential of these extracts.

The production of tBID in the extrinsic pathway may affect the intrinsic pathway. Therefore, we evaluated the mRNA levels of BAX, p53, and Bcl-2, which are involved in the intrinsic pathway. Figure 7 shows the temporal mRNA levels of Bcl-2, BAX, and p53 in HeLa cells as assessed by qRT-PCR. Interestingly, Bcl-2 mRNA level increased with time in cells treated with the HE, DME, or CE extract, and after 10 h, 2.5-, 4.3-, and 4.5-folds

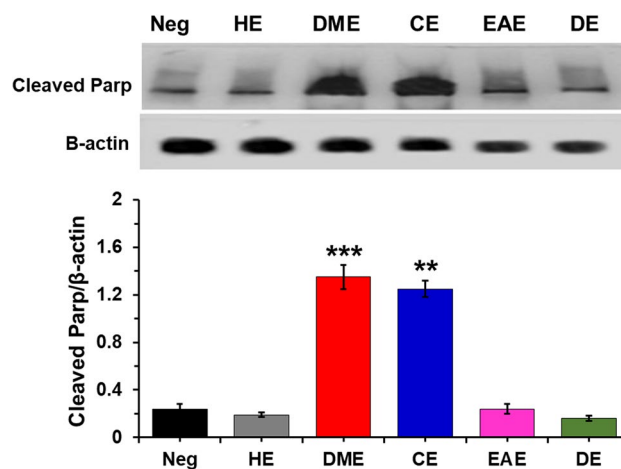


Figure 6. Evaluation of the cleaved Parp level in the HeLa cells treated with extracts of *M. glyptostroboides* extracts (50 µg/ml). ** $p < 0.01$ and *** $p < 0.001$ indicates statistical significances compared to negative control.

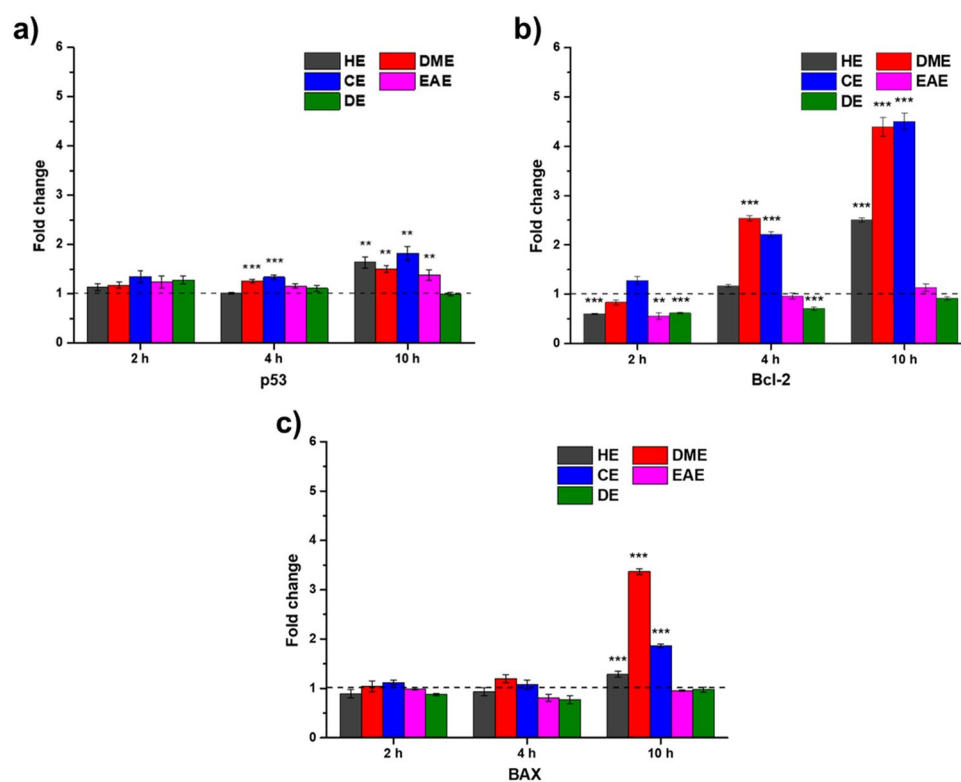


Figure 7. Gene expression analysis in HeLa cells. (a) *p53*, (b) *Bcl-2*, and (c) *BAX* expression. ** $p < 0.01$ and *** $p < 0.001$ indicates statistical significances compared to negative control.

increase were observed, respectively, relative to the level in the negative control group. After 10 h of treatment with the HE, CE, or DME extract, BAX mRNA level was upregulated by 1.3-, 1.9-, and 3.4-folds, respectively. Additionally, p53 mRNA level increased approximately 1.5-fold upon 10 h of treatment with the HE, DME, or CE extract (Fig. 7a). However, no significant changes were observed with the EAE and DE extracts. BAX mRNA level was increased by the DME and CE extracts in a time-dependent manner, but Bcl-2 mRNA level also increased (Fig. 7b,c). Both BAX and Bcl-2 are involved in the intrinsic apoptosis pathway. BAX is a pro-apoptotic protein regulated by the tumor suppressor protein p53. Conversely, Bcl-2 is an anti-apoptotic protein that binds to BAX. When HeLa cells were treated with the HE, DME, and CE extracts, the intrinsic pathway was distracted by the upregulated p53 levels while being induced by the upregulated p53 and BAX levels. In addition, reactive oxygen species, which is one of the major factors in the intrinsic apoptosis pathway, was found to be different at the chemical level, however, it did not cause any difference in the cells (Supplementary Fig. S3).

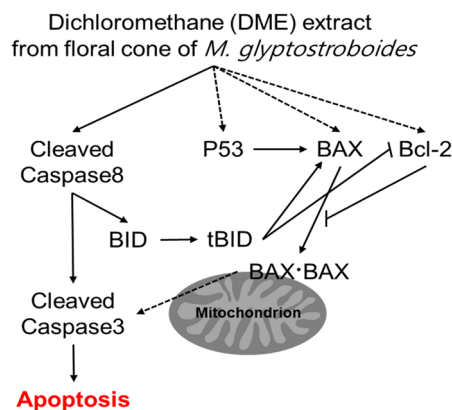


Figure 8. Working model for the mechanism underlying the induction of apoptosis in HeLa cells by the DME extract. The dotted arrows indicate that more evidence is needed to establish a correlation. The solid arrows denote activation. "—" indicates inhibition.

Taken together, *M. glyptostroboides*-derived organic extracts, particularly the DME extract, which may contain anticancer terpenoid compounds¹³ induced Cl Cas8, resulting in the increased cleavage of BID into tBID, which probably promotes the intrinsic pathway. However, Bcl-2, which increases simultaneously with BAX and p53 levels, is thought to interfere with the intrinsic pathway (Fig. 8).

Conclusions

The DME organic extract derived from the floral cones of *M. glyptostroboides* containing anticancerous quinone, terpenes and steroid components showed high cytotoxicity in cervical cancer cells (HeLa) and low toxicity in normal cells (COS7). Furthermore, Hoechst 33342 staining, cell cycle assay, western blotting, and RT-PCR results showed that the cytotoxicity of the extract resulted from the induction of the extrinsic apoptosis pathway. In particular, cleaved Cas8, which plays an important role in extrinsic apoptosis, was upregulated by 27.17-fold relative to the level in the negative control, indicating the anticancer potential of the DME extract. However, further research is needed to unravel the death receptor and corresponding extrinsic pathway to elucidate the exact apoptosis mechanism induced by the DME extract and the relevant biomedical potential.

Data availability

The authors declare that all the data supporting the finding of this study are available within the article and from the corresponding author on reasonable request.

Received: 9 June 2020; Accepted: 30 November 2020

Published online: 13 January 2021

References

1. Moon, E. K. *et al.* Trends and age-period-cohort effects on the incidence and mortality rate of cervical cancer in Korea. *Cancer Res. Treat.* **49**, 526–533 (2017).
2. Lin, C. J. *et al.* Integrated self-assembling drug delivery system possessing dual responsive and active targeting for orthotopic ovarian cancer theranostics. *Biomaterials* **90**, 12–26 (2016).
3. Moss, C. & Kaye, S. B. Ovarian cancer: Progress and continuing controversies in management. *Eur. J. Cancer* **38**, 1701–1707 (2002).
4. Bast, R. C., Hennessy, B. & Mills, G. B. The biology of ovarian cancer: New opportunities for translation. *Nat. Rev. Cancer* **9**, 415–428 (2009).
5. Ulbrich, K. *et al.* Interaction of folate-conjugated human serum albumin (HSA) nanoparticles with tumour cells. *Int. J. Pharm.* **406**, 128–134 (2011).
6. Jeong, H. *et al.* Photosensitizer-conjugated human serum albumin nanoparticles for effective photodynamic therapy. *Theranostics* **1**, 230–239 (2011).
7. Du, C. *et al.* A pH-sensitive doxorubicin prodrug based on folate-conjugated BSA for tumor-targeted drug delivery. *Biomaterials* **34**, 3087–3097 (2013).
8. Pfeffer, C. M. & Singh, A. T. K. K. Apoptosis: A target for anticancer therapy. *Int. J. Mol. Sci.* **19**, 448 (2018).
9. Kiraz, Y., Adan, A., Kartal Yandim, M. & Baran, Y. Major apoptotic mechanisms and genes involved in apoptosis. *Tumor Biol.* **37**, 8471–8486 (2016).
10. Bajpai, V. K., Yoon, J. I. & Chul Kang, S. Antioxidant and antidermatophytic activities of essential oil and extracts of *Metasequoia glyptostroboides* Miki ex Hu. *Food Chem. Toxicol.* **47**, 1355–1361 (2009).
11. Bajpai, V. K. & Kang, S. C. Antifungal activity of leaf essential oil and extracts of *Metasequoia glyptostroboides* Miki ex Hu. *JAOCs J. Am. Oil Chem. Soc.* **87**, 327–336 (2010).
12. Bajpai, V. K. & Kang, S. C. Tyrosinase and α -glucosidase inhibitory effects of an abietane type diterpenoid taxodone from *Metasequoia glyptostroboides*. *Natl. Acad. Sci. Lett.* **38**, 399–402 (2015).
13. Bajpai, V. K., Rather, I. A., Kang, S. C. & Park, Y. H. A diterpenoid taxoquinone from *Metasequoia glyptostroboides* with pharmacological potential. *Indian J. Pharm. Educ. Res.* **50**, 458–464 (2016).
14. Bajpai, V. K. *et al.* Characterization and antibacterial potential of lactic acid bacterium *Pediococcus pentosaceus* 4I1 isolated from freshwater fish *Zacco koreanus*. *Front. Microbiol.* **7**, 2037 (2016).

15. Khan, I., Bahuguna, A., Kumar, P., Bajpai, V. K. & Kang, S. C. In vitro and in vivo antitumor potential of carvacrol nanoemulsion against human lung adenocarcinoma A549 cells via mitochondrial mediated apoptosis. *Sci. Rep.* **8**, 144 (2018).
16. Lee, H. *et al.* Design and development of caffeic acid conjugated with: *Bombyx mori* derived peptide biomaterials for anti-aging skin care applications. *RSC Adv.* **7**, 30205–30213 (2017).
17. Xiong, W., Gong, J. & Xing, C. Ferruginol exhibits anticancer effects in OVCAR-3 human ovary cancer cells by inducing apoptosis, inhibition of cancer cell migration and G2/M phase cell cycle arrest. *Mol. Med. Rep.* **16**, 7013–7017 (2017).
18. Liu, Y.-L. *et al.* Taxodione and arenarone inhibit farnesyl diphosphate synthase by binding to the isopentenyl diphosphate site. *Proc. Natl. Acad. Sci.* **111**, E2530–E2539 (2014).
19. Gupta, A. *et al.* Design, synthesis and biological evaluation of estradiol–chlorambucil hybrids as anticancer agents. *Bioorg. Med. Chem. Lett.* **20**, 1614–1618 (2010).
20. Shanthi, M. P. *et al.* In vitro anticancer activity of *Biophytum sensitivum* whole plant extracts against cervical and liver cancer cell lines. *Int. J. Pharm. Sci. Res.* **7**, 5128–5135 (2016).
21. Amna, U. Evaluation of cytotoxic activity from Temurui (*Murraya koenigii* [Linn.] Spreng) leaf extracts against HeLa cell line using MTT assay. *J. Adv. Pharm. Technol. Res.* <https://doi.org/10.4103/japtr.JAPTR> (2019).
22. Ziegler, U. & Groscurth, P. Morphological features of cell death. *News Physiol. Sci.* **19**, 124–128 (2004).
23. Chothiphirat, A., Nittayaboon, K., Kanokwiroon, K., Srisawat, T. & Navakanitworakul, R. Anticancer potential of fruit extracts from *Vatica diospyroides* symington type SS and their effect on program cell death of cervical cancer cell lines. *Sci. World J.* **2019**, 1–9 (2019).
24. Qi, L. *et al.* Folate-modified bexarotene-loaded bovine serum albumin nanoparticles as a promising tumor-targeting delivery system. *J. Mater. Chem. B* **2**, 8361–8371 (2014).
25. Kantari, C. & Walczak, H. Caspase-8 and Bid: Caught in the act between death receptors and mitochondria. *Biochim. Biophys. Acta Mol. Cell Res.* **1813**, 558–563 (2011).
26. Boulares, A. H. *et al.* Role of poly(ADP-ribose) polymerase (PARP) cleavage in apoptosis. *J. Biol. Chem.* **274**, 22932–22940 (1999).

Acknowledgements

This study was supported by a grant of the Korea Industrial Complex Corp. (KICOX, No. RIC20001).

Author contributions

H.L., S.K., H.K.K., D.K.D. and C.O. performed the research, H.L., C.O. and V.K.B conceived and designed the experiments. H.L. and V.K.B. wrote the manuscript. V.K.B., Y.K.H. and Y.S.H. evaluated the initial draft of the manuscript. V.K.B. and Y.S.H. approved the manuscript for submission.

Competing interests

The authors declare no competing interests.

Additional information

Supplementary Information The online version contains supplementary material available at <https://doi.org/10.1038/s41598-020-79573-8>.

Correspondence and requests for materials should be addressed to V.K.B., Y.-K.H. or Y.S.H.

Reprints and permissions information is available at www.nature.com/reprints.

Publisher's note Springer Nature remains neutral with regard to jurisdictional claims in published maps and institutional affiliations.



Open Access This article is licensed under a Creative Commons Attribution 4.0 International License, which permits use, sharing, adaptation, distribution and reproduction in any medium or format, as long as you give appropriate credit to the original author(s) and the source, provide a link to the Creative Commons licence, and indicate if changes were made. The images or other third party material in this article are included in the article's Creative Commons licence, unless indicated otherwise in a credit line to the material. If material is not included in the article's Creative Commons licence and your intended use is not permitted by statutory regulation or exceeds the permitted use, you will need to obtain permission directly from the copyright holder. To view a copy of this licence, visit <http://creativecommons.org/licenses/by/4.0/>.

© The Author(s) 2021